KU Leuven
Department of Mechanical Engineering
Celestijnenlaan 300 - box 2420
B-3001 Heverlee (Belgium)

Proceedings of

ISMA2020

International Conference on
Noise and Vibration Engineering

USD2020

International Conference on
Uncertainty in Structural Dynamics

7 to 9 September, 2020
Editors: W. Desmet, B. Pluymers, D. Moens, S. Vandemaele.

Proceedings of

ISMA2020

International Conference on

Noise and Vibration Engineering

USD2020

International Conference on

Uncertainty in Structural Dynamics

Leuven
7 to 9 September, 2020

Organising Committee:

Prof. Dr. ir. W. Desmet,	*ISMA Conference Chairman*
Dr. ir. B. Pluymers,	*ISMA Conference Chairman*
Prof. Dr. ir. P. Sas,	*ISMA Honorary Chairman*
Prof. Dr. ir. D. Moens,	*USD Conference Chairman*
Prof. Dr. ir. D. Vandepitte,	*Programme Chairman*
Prof. Dr. ir. W. De Roeck,	*Conference Programme*
Prof. Dr. ir. K. Gryllias,	*Conference Programme*
ir. S. Vanpaemel,	*Conference Manager*
ir. R. Adduci,	*Technical Manager*
Mrs. L. Notré,	*Conference Secretary*
ir. S. Vandemaele,	*Conference Proceedings and database*
ir. J. Kersschot,	*Exhibition*
ir. A. Angeli,	*Public Relations*
ing. O. Van Dessel,	*Social Events*
ir. S. Ahsani,	*Webmaster*

Organised by:

KU Leuven – Department of Mechanical Engineering
Celestijnenlaan 300 - box 2420
B-3001 Heverlee (Belgium)

ISBN 9789082893113

ISMA2020 PAPERS

AVC

Session Active Vibration Control

AE

Session Aero-Elasticity

AA

Session Aeroacoustics and flow noise

CAM

Session Characterisation, design and optimisation of vibro-acoustic materials and structures

CMRM

Session Condition monitoring of rotating machinery

D

Session Damping

DT

Session Dynamic testing: methods and instrumentation

JOINT

Session Dynamics of Joints

RMD

Session Dynamics of Rotating Machinery

CIV

Session Dynamics of civil structures

INV

Session Inverse Methods - Load Identification

MHF

Session Medium and High Frequency Techniques

MTC

Session Modal testing: methods and case studies

MOR

Session Model Order Reduction

MU

Session Model Update

MB

Session Multi-body dynamics and control

NL

Session Non-linearities: identification and modelling

OMCV

Session Optical Methods and Computer Vision for Vibration Engineering

PBNV2

Session Pass by noise

RAIL

Session Railway dynamics and ground vibrations

SD

Session Structural dynamics: methods and case studies

SHM

Session Structural health monitoring (Structures)

SC

Session Substructuring and Coupling

TVD

Session Tuned Vibration Absorbers and Dampers

NVH

Session Vehicle noise and vibration (NVH)

VAM

Session Vibro-acoustic modelling and prediction

WIND

Session Wind turbine dynamics

USD2020 PAPERS

USDUIQ

Session USD - Uncertainty Identification and Quantification

USDMP

Session USD - Uncertainty modelling and propagation

USDA

Session USD – Applications

A numerical model for NVH analysis of gearboxes employed on agricultural equipment

A. Gabrielli [1], **F. Pizzolante** [1], **E. Soave** [1], **M. Battarra** [1], **C. Mazzeo** [2], **M. Tarabra** [2], **E. Fava** [3], **E. Mucchi** [1]

[1] University of Ferrara, Department of Engineering
Via Saragat, 1, Ferrara – 44122, Italy
e-mail: **alberto.gabrielli@unife.it**

[2] FEV Italia S.r.l.
Via Borsellino, 38/16, Torino - 10138, Italy

[3] Comer Industries S.p.a
Via Magellano, 27, Reggiolo (RE) - 42026, Italy

Abstract

The aim of this paper is to describe a numerical vibro-acoustic methodology, experimentally assessed, for the estimation of the overall vibratory and acoustic level of a gearbox employed on agricultural equipment. The process is carried out in order to create the NVH digital twin of the real gearbox. The vibro-acoustic model is the combination of three sub-models: a lumped-parameter (LP) model, a structural finite-element (SFE) model and an acoustical finite-element (AFE) model. The LP model is used to obtain the reaction forces on the bearings during working conditions. Reaction forces are employed as an input for the further SFE dynamic model to evaluate the dynamic response of the gearbox's case, which is the only meshed part. The dynamic response is exploited to set-up an AFE model which allows to estimate the noise generation in terms of overall acoustic pressure. The numerical simulation results are validated using experimental data acquired on a real gearbox. Testing activities have been carried out at Comer Industries facility in Reggiolo, where specimens and test benches have been set. Advantages and limitations of the model are reported.

1 Introduction

High levels of noise may be produced by a gearbox during its operational life. The noise is generated by gear meshing, and it is further amplified by the resonances of the case [1]. Since it may be difficult to estimate the acoustic emission during the design process, which is finalized at obtaining a certain gear ratio for the gearbox, noise levels may be too high and exceed acoustic tolerance limits. The overall acoustic pressure level, in fact, will depend both on the choice of the gears and on the properties of the case. Assuming that the design of the case is fixed (i.e. it is already optimized in terms of geometry and material), one may propose many designs for the gears, e.g. different teeth profiles or gear types, in order to obtain the lowest noise generation possible while achieving the required gear ratio. This goal can be accomplished by performing an extensive campaign of experimental testing, but this means that every possible combination of gears and teeth profile has to be tested, and the acoustic pressure levels must be measured for each one of them. The process is very time-consuming and requires a large amount of resources. A faster way to optimize the design consists in generating a digital twin of the gearbox, i.e. a digital replication of the physical entity [2] allowing to test different gear configurations without creating a physical prototype of the gearbox for each test. In this case, the experimental tests must be carried out only to validate the baseline model: design modifications, then, may be numerically evaluated by changing its input parameters. Within this framework, this paper describes the generation of a digital twin of a real gearbox employed on agricultural equipment,

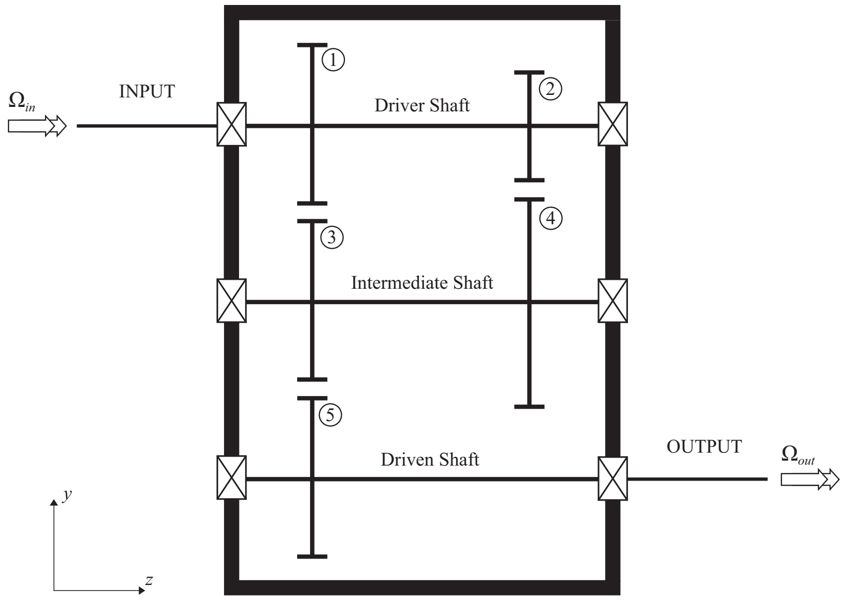

Figure 1: Gearbox schematic diagram

aiming at evaluating the overall acoustics in operational conditions. The system under study is schematically depicted in Figure 1. The gearbox case contains three shafts, five gears and six bearings. The shafts name driver, intermediate and driven shafts, while the gears are denoted by numbers from 1 to 5. Gear ratio of the system $\tau = \Omega_{out}/\Omega_{in}$ may take the values 1 or 1.8, depending on the meshing gears: τ is equal to 1 when the meshing takes place between gears 1-3 and 3-5, while $\tau = 1.8$ when the meshing occurs between gears 2-4 and 3-5. The gear ratio may be changed by using a coupling mounted on the driver shaft. In this work, results will be reported only for $\tau = 1$, meaning that the output speed has to be equal to the input speed so that $\Omega_{in} = \Omega_{out}$. This gear ratio is achieved due to the fact that gears 1, 3 and 5 have the same number of teeth (37). The proposed digital twin is a combination of a lumped-parameter (LP) model, a structural finite-element (SFE) model and an acoustical finite-element (AFE) model. A similar procedure, involving the use of these three types of models, has been already developed by one of the authors in previous works ([3][4]), and also by other researchers ([5]). In the following, after a brief description of the experimental setup, the models are presented and experimentally assessed.

2 Experimental setup

The gearbox used for the tests is shown in Figure 2. The driver shaft is connected to the output shaft of the engine of an agricultural tractor by an universal joint, while the driven shaft is connected to a braking system. The case is fixed on a steel plate. The reference frame depicted in the bottom left of the figure, employed for the experimental tests, is the same used for all the numerical models. The performed experimental tests may be divided in two categories: experimental modal analysis (EMA) and operative analysis. The EMA has been carried out by using 31 excitation points and 3 response points distributed on the surfaces of the case, by using the roving hammer based method. The excitations have been applied with an impact hammer model PCB 086D05, while the responses have been measured by piezoelectric triaxial accelerometers model PCB 356B21. The results of this analysis are used to validate the SFE model. The operative analysis has been realized in firing condition by applying a load on the driver shaft through the output shaft of the engine. Acceleration on the case has been measured by using two piezoelectric triaxial accelerometers model PCB 356B21 (Acc1 and Acc2 in Figure 2) fixed on two opposite faces of the case, and the acoustic pressure has been measured with two microphones model PCB 378B02 in front of the accelerometers, at a distance of 20 cm from the corresponding surfaces (Mic1 and Mic2 in Figure 2). The rotational speed of the input and output shafts have been evaluated by using two optical tachometers placed on the corresponding shafts. Tests have been run for one working condition, and for two different teeth profiles, here called *Baseline* and

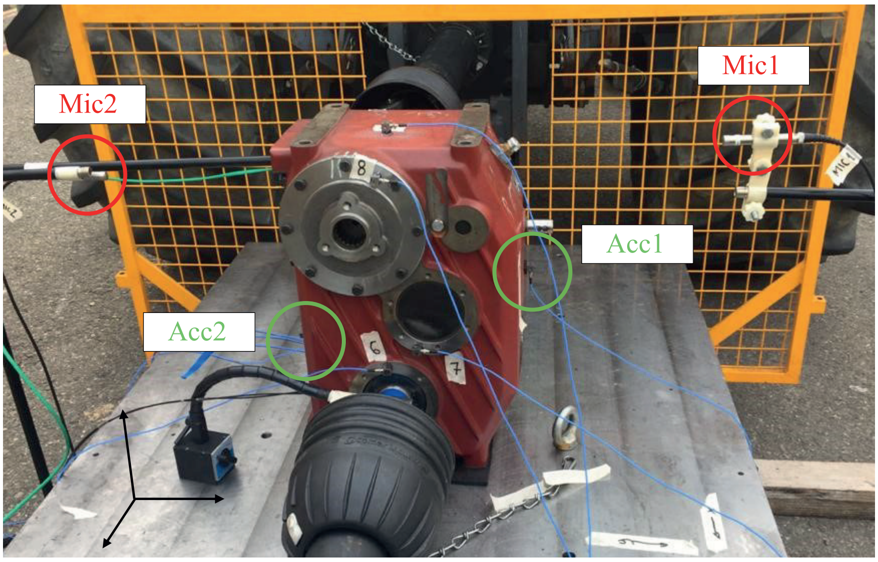

Figure 2: Experimental setup.

Mod1. The latter consists in a modification of the geometry of the former, i.e. the original profile, but is not described for confidentiality reasons. By changing the profiles, two different time-varying meshing stiffness are generated, hence producing different acoustic emissions. The working condition for which the system has been tested is reported in Table 1 and it is defined by rotational speed of the driver shaft Ω_{in}, input power P and gear ratio τ. The rotational frequency f_r of the shafts and the gear meshing frequency f_g of gears 1-3 and 3-5 are also given. Notice that for both of them only one value is listed since for $\tau = 1$ all shafts have the same speed and the gear meshing frequency is identical for both gear pairs. Pressure levels are reported in Figure 3 for both tested profiles. From these graphs it may be noticed how the highest contribution to the overall level comes from the frequency interval consisting in the 1/3 octave bands whose center frequencies range from 630 Hz to 2500 Hz, i.e. from 562 Hz (lower frequency limit of the 630 Hz band) to 2818 Hz (upper frequency limit of the 2818 Hz band). This result allows lowering the computational burden for the SFE and AFE dynamic model by reducing the frequency range of the analysis from 0 - 20 kHz to the reduced interval 562 - 2818 Hz. Furthermore, it must be noted that by changing teeth profile from *Baseline* to *Mod1* the overall levels decrease, as reported in Table 2.

3 Description of the models and experimental validation

The developed digital twin is a combination of three sub-models: a LP model, a SFE model and an AFE model of a gearbox employed on agricultural equipment. The output of the combined LP/SFE/AFE model is the overall acoustic pressure due to specified working conditions and gear design. The LP model allows to estimate the reaction forces on the bearings due to gear meshing by simulating the dynamic effect of the motion of the components inside the case. It is a non-linear model, as it takes into account the transmission error, gear pair backlash, meshing stiffness, bearing stiffness and damping. For the latter, values are chosen in order to consider the damping effect of the oil inside the case. Frequency-dependent reaction forces are the input of the dynamic model. In the SFE model, only the case is meshed. All the internal components are substituted by concentrated masses connected to the bearing housings by rigid elements. The SFE model was validated by performing a numerical modal analysis on the frequency range of interest, and comparing the obtained natural frequencies and mode shapes with the results assessed by the experimental modal analysis. The examined frequency interval is the one with the highest acoustic emission as determined by experimental measurements. Then, the same validated mesh is used to carry out a dynamic analysis where the input forces are the ones obtained by the LP model and applied on the bearing housings. It is assumed that case vibration, which is the output of the SFE model, has no influence on the dynamic behavior of the moving components. The output of the SFE the model is exploited as input for the AFE model, which employs the acoustic transfer

Table 1: Tested working conditions.

Quantity	Value	Description
P	50 kW	Input power
τ	1	Gear ratio
Ω_{in}	506.4 RPM	Rotational speed of the driver shaft
Ω_{out}	506.4 RPM	Rotational speed of the driven shaft
f_r	8.4 Hz	Rotational frequency of the driver, intermediate and driven shafts
f_g	310.8 Hz	Meshing frequency of gear pairs 1-3 and 3-5
Teeth profiles	Baseline, Mod1	Names of the tested profiles

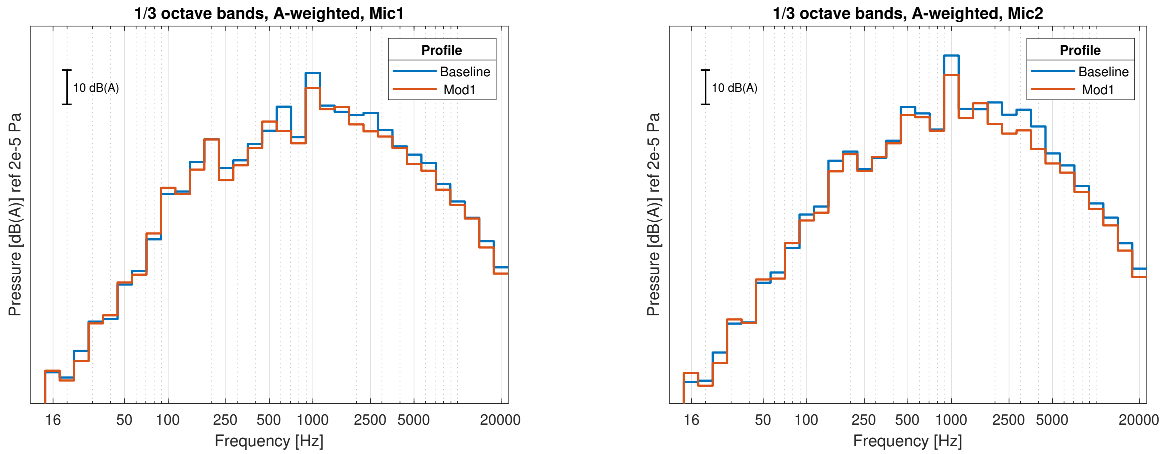

(a) Microphone 1

(b) Microphone 2

Figure 3: Acoustic levels sensed by the microphones for both tested profiles. Reference pressure is $p_{ref} = 2 \cdot 10^{-5}\ Pa$.

Table 2: Reduction of the overall acoustic pressure levels due to change of the teeth profile. The levels are A-weighted and computed over the reduced frequency range 562 - 2818 Hz. Reference pressure is $P_{ref} = 2 \cdot 10^{-5}\ Pa$.

	Mic1	Mic2
dB(A) reduction	-3.5	-4.9

vector (ATV) method to evaluate the overall acoustic pressure at specified locations due to the vibration of the case. Both the SFE and the AFE models are developed using Simcenter 3D as the pre/post processor and Simcenter Nastran as the solver [6]. The LP model is developed in MATLAB [7]. Experimental assessment is carried out by means of experimental modal analysis (EMA) as well as acceleration and acoustic pressure measurements.

3.1 Lumped parameter model

The dynamic behavior of the moving components inside the case is described by means of a non-linear lumped-parameter model. The LP model consists in the subdivision of the system into masses and inertias connected to each other by elastic and viscous damping elements. The model considers the effects of time-varying mesh stiffness, the non-linearity of the meshing phenomenon and a constant bearing stiffness. During the meshing, the existence of backlash is necessary to allow better lubrication, reduce wear and limit interference due to geometrical construction errors. The backlash induces torsional vibrations that can cause the detachment between teeth [8]. Given a direction of pinion rotation, the forces are exchanged along the direct line of action. If contact is lost, the driven wheel may impact the pinion on the opposite side of the tooth. Considering that only spur gears are present in the system, translations and rotations were monitored just in the plane transverse to the gears, no displacement will occur in the z direction. In fact, according to Figure 4 the LP model has nine degrees of freedom: the x and y translations and the angular displacement θ around the rotation axis for each gear. The values assigned to the components are listed in Table 3. Since the tested configuration has a gear ratio $\tau = 1$, the considered gears are 1, 3 and 5 (see Figure 1). The equation governing the motion of the system is:

$$[M]\{\ddot{x}\} + f(x_r, x_b)\left[[C]\{\dot{x}\} + [K]\{x\} - \frac{1}{2}\{k_m\}x_b\right] = \{F\} \tag{1}$$

where

$$f(x_r, x_b) = \begin{cases} 1, & \text{if} \quad x_r > \frac{x_b}{2} \\ 0, & \text{if} \quad -\frac{x_b}{2} \le x_r \le \frac{x_b}{2} \\ -1, & \text{if} \quad x_r < -\frac{x_b}{2} \end{cases} \tag{2}$$

and $[M]$, $[C]$ and $[K]$ are the mass, damping and stiffness matrices, respectively; x_r is the dynamic transmission error; x_b is the gear backlash; $\{k_m\}$ is the time-varying meshing stiffness; $\{\ddot{x}\}$, $\{\dot{x}\}$, $\{x\}$ are the acceleration, velocity and displacement vectors; $\{F\}$ is the external forces vector. Damping is defined as Rayleigh damping, i.e. proportional to mass and stiffness matrices, so that:

$$[C] = \alpha[M] + \beta[K] \tag{3}$$

Different strategies can be followed on the choice of α and β coefficients: in the first instance, they may be fixed according to experience. Then, they may be calibrated on the most important (linearized) resonances of the geartrain (experimentally evaluated for example). In this study the first option was adopted. Different damping coefficients were considered for each damper of the LP model, the chosen values are shown in Table 3. As depicted in Figure 2, lumped parameter m_i represents the oscillating mass of all the elements fixed to the i-th shaft, while J_i considers the inertia of all rotating elements. When meshing takes place between gears 1 and 3, gear 2 is not rotating with the driver shaft. Its rotary motion is accomplished by gear 4 that is fixed to the intermediate shaft. Thus, the rotary inertia of gear 2 is considered as part of $J_{intermediate}$. On the other hand, looking at the radial displacement, the oscillating mass of gear 2 is part of m_{driver}. The numerical analysis was carried out by using MATLAB. Simulations have been run for one working condition, shown in Table 1, and for two different teeth profiles *Baseline* and *Mod1*, which generate two different time-varying meshing stiffness, as reported in Table 3. Reaction forces on the bearing are exported and used as input solicitation for the SFE analysis. Results are shown in Figure 5. It is worth noting that there is a strong reduction of bearing reaction forces due to the tooth profile modification.

3.2 Structural finite-element model of the gearbox case

A finite-element analysis is carried out in order to estimate the case vibration due to reaction forces generated by gear meshing and acting on the bearings. In the SFE model, only the external case of the gearbox is meshed by using 4-nodes 3D tetrahedral elements. On the contrary, all the internal components are replaced by concentrated masses, defined only by their center of mass and inertial properties (mass and moments of inertia). These concentrated masses are connected to the bearing housings by rigid elements as depicted in Figure 6: the central node, which is the concentrated mass, is connected to all the nodes on the surface of the corresponding bearing housing. Concerning the boundary conditions, fixed constraints are applied on the bottom of the case, in place of the screws that would tighten it to the plate below. A fixed constraint implies that all the degrees of freedom for the involved nodes are restrained. As for the material, the case is made of cast iron with Young's modulus $E = 90\ GPa$ and density $\rho = 7250\ kg/m^3$.

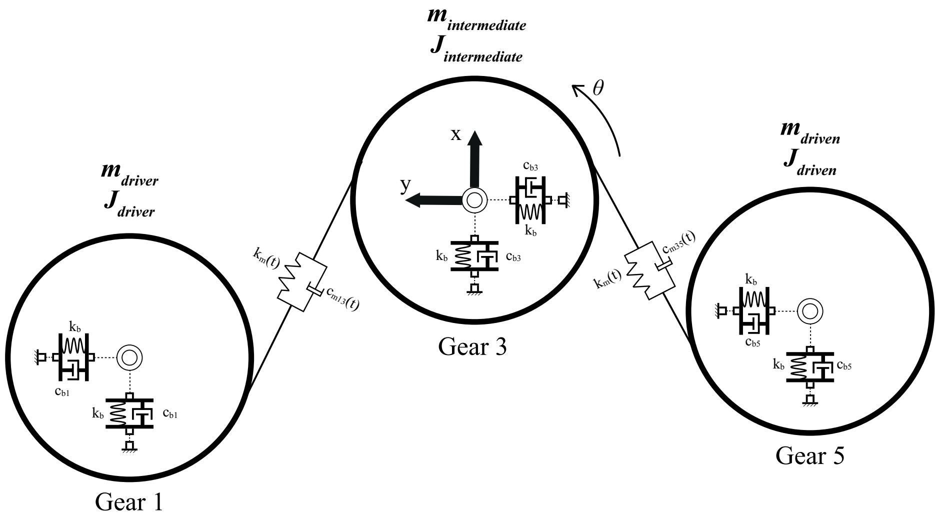

Figure 4: Lumped parameter (LP) model schematic.

Table 3: Values assigned to the components of the LP model.

Quantity	Value	Description
m_{driver}	$15.88\ kg$	Mass of the driver shaft
$m_{intermediate}$	$16.85\ kg$	Mass of the intermediate shaft
m_{driven}	$10.69\ kg$	Mass of the driven shaft
J_{driver}	$2.36 \cdot 10^4\ kg \cdot mm^2$	Moment of inertia of the driver shaft
$J_{intermediate}$	$5.38 \cdot 10^4\ kg \cdot mm^2$	Moment of inertia of the intermediate shaft
J_{driven}	$1.72 \cdot 10^4\ kg \cdot mm^2$	Moment of inertia of the driven shaft
k_b	$1.82 \cdot 10^9\ N/m$	Bearing stiffness
$k_{m,Baseline}$	$7.73 \cdot 10^8\ N/m$	Average value of the meshing stiffness of *Baseline* profile
$k_{m,Mod1}$	$7.26 \cdot 10^8\ N/m$	Average value of the meshing stiffness of *Mod1* profile

The structural FE mesh, which will be later used in the dynamic model, is validated against the data collected with the EMA by comparing the natural frequencies and the mode shapes numerically evaluated by using the Nastran solution SOL 103. It has been decided to focus only on the frequency range with the highest acoustical emission, which is located between 562 and 2818 Hz as assessed by the experimental measurements reported in Section 2, and in particular on the first two experimental modes in this interval, found at 828 Hz and 1221 Hz. The results obtained with SOL 103 are reported in Table 5. The numerical and experimental mode shapes are shown in Figure 7a for the first mode and Figure 7b for the second mode. It is worth nothing that, for both modes, the obtained numerical natural frequencies are close to the experimental ones, as the frequency difference between them is 0.9 % for mode 1 and 6.4 % for mode 2. Furthermore, the modal assurance criterion (MAC) takes fairly high values for both of them, since it is equal 0.66 and 0.73 for the first and second mode, respectively. These results denote a good accordance between the experimental and numerical results, hence validating the SFE model and allowing to further employ it for the dynamic analysis.

The dynamic model is developed using the same mesh generated for the modal analysis. This time, the modal frequency response solution (SOL 111 in Nastran) is employed. Forces are applied on the bearing housings (Figure 8) by providing their magnitude and phase, and distributed on the entire surface for each housing. Since the axial forces are neglected, a total of twelve forces acting on the system, six of them in the x direction and the other six in the y direction, are considered so that two forces acting on each bearing are accounted. To accomplish this, each one of the forces depicted in Figure 5 is divided between the two bearings of each

Table 4: Damping coefficients for the LP model.

Parameter		$\alpha\ [s^{-1}]$	$\beta\ [s]$
C_{b1}	Driver Bearing	1	$1 \cdot 10^{-4}$
C_{m13}	Driver - Intermediate meshing	1	$5 \cdot 10^{-4}$
C_{b3}	Intermediate bearing	1	$5 \cdot 10^{-4}$
C_{m35}	Intermediate - Driven Bearing	1	$5 \cdot 10^{-4}$
C_{b5}	Driven Bearing	1	$6 \cdot 10^{-4}$

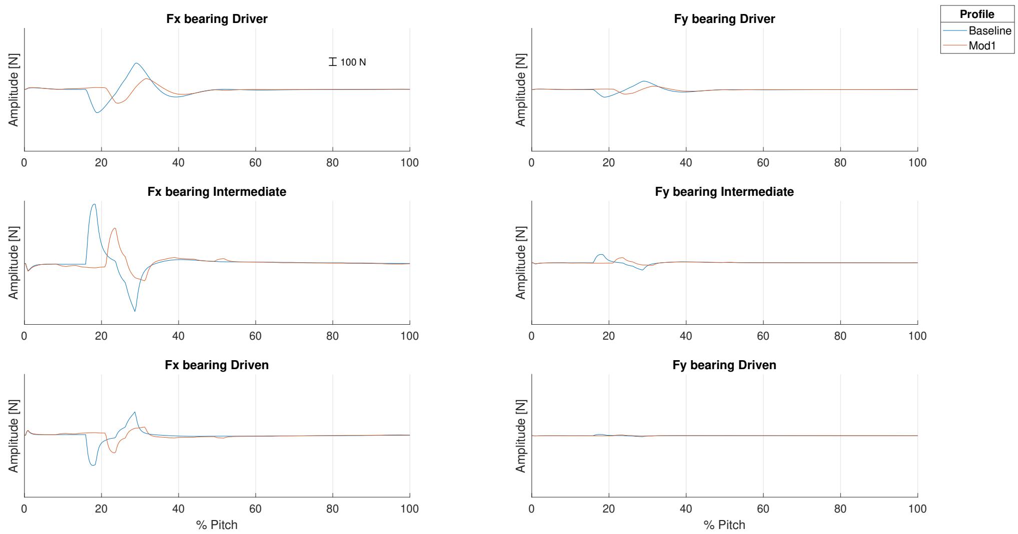

Figure 5: Bearing reaction forces.

shaft, scaling its magnitude based on the distance of the meshing gear from the corresponding bearing. As for the modal analysis, the frequency range of interest is again the one that has been assessed to have the highest acoustical emission, located between 562 and 2818 Hz. Hence, the dynamic analysis is carried out only in this frequency range. Furthermore, frequency-dependent modal damping is introduced. Its values, estimated by the EMA, are reported in Table 6. The applied forces are the ones estimated by the LP model for the working conditions reported in Table 1. The output of the model of major interest is the vibration of the case, namely its acceleration. To validate the results, numerical acceleration results are compared with experimental results obtained during the operative analysis by the accelerometers Acc1 and Acc2 (Figure 2). Acceleration is evaluated numerically by taking the *x* component of the acceleration from two nodes on the case, located in the same position as the accelerometers in Figure 2. These two nodes are shown in Figure 9. Results are compared in terms of reduction of overall acceleration levels in the frequency range 562 - 2818 Hz as reported in Table 7 and in 1/3 octave band spectrum as shown in Figure 10. The dynamic model is able to capture the reduction due to the modified profile, as the order of magnitude of the reductions is similar for both accelerometers: for the accelerometer Acc1, in fact, the model predicts a reduction of 7.3 dB, while the real reduction is -5.3 dB; for Acc2 the results are closer, as the model gives a reduction of 5.5 dB against the experimental reduction of 6.1 dB. Since we are interested in the assessment of the overall levels, these results validate the dynamic model and its output may be used as the input for the AFE model.

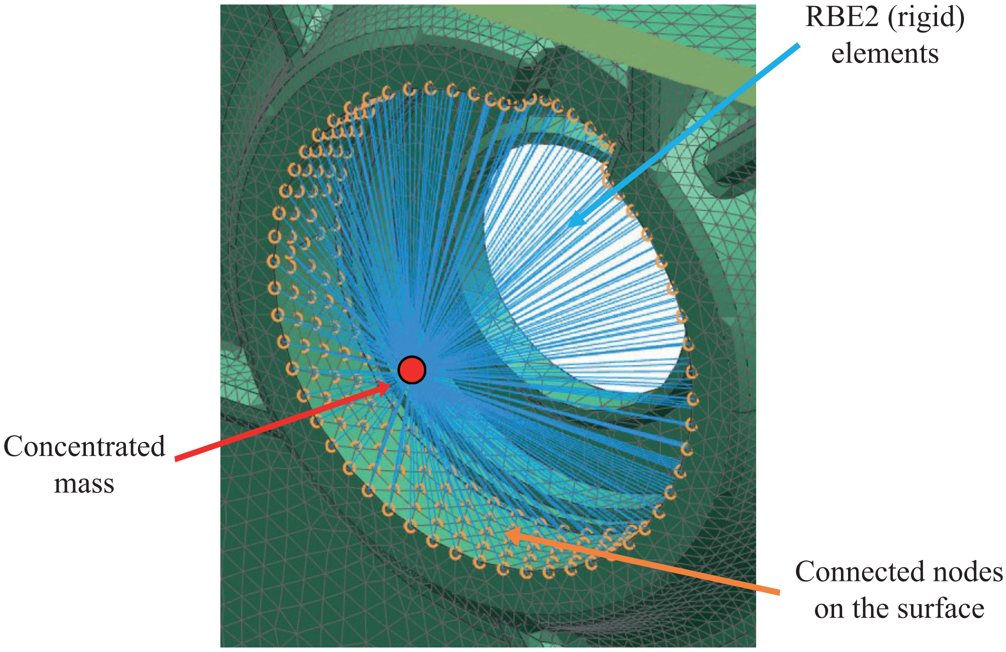

Figure 6: Rigid elements connecting a concentrated mass to the case.

Table 5: Comparison between the first two natural frequencies obtained experimentally (EMA) and numerically (SOL 103).

	Natural Frequency [Hz]		
	EMA	Numerical	MAC
Mode 1	828	835	0.66
Mode 2	1221	1143	0.73

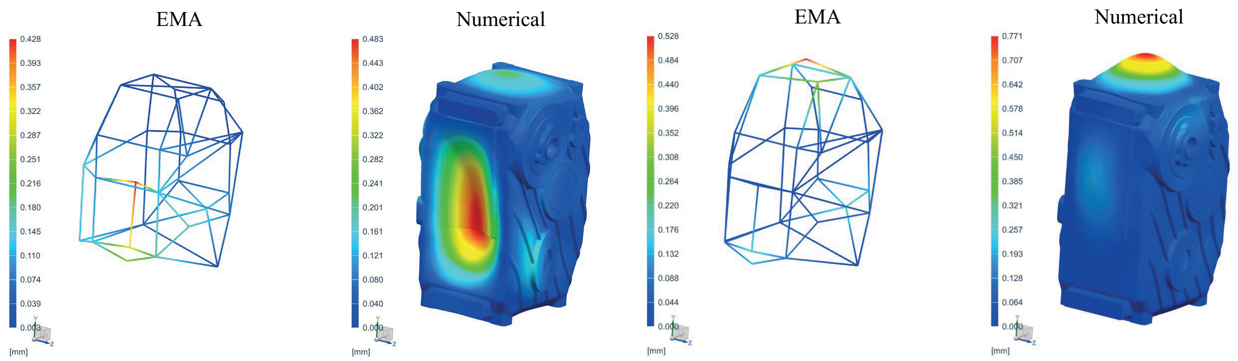

(a) Mode 1 (b) Mode 2

Figure 7: Comparison between the first two mode shapes obtained experimentally (EMA) and numerically (SOL 103).

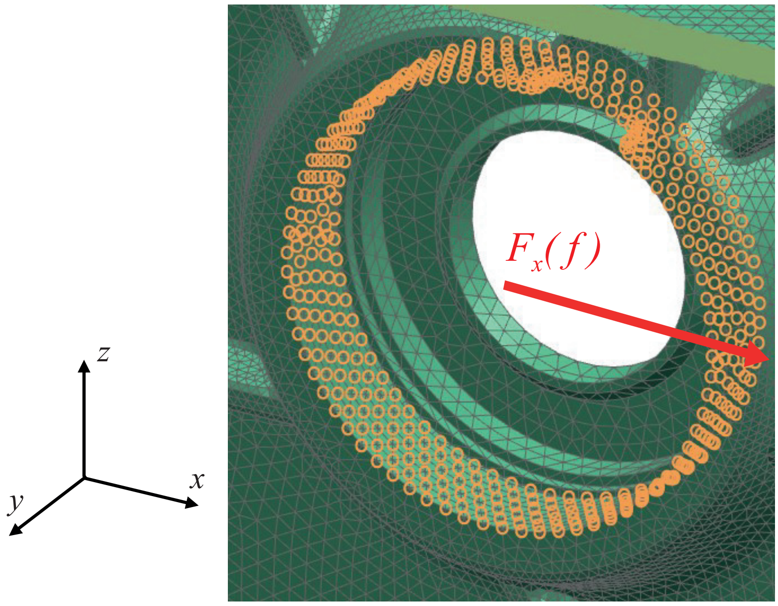

Figure 8: Force on the bearing of the driver shaft, acting on the highlighted orange nodes. In the figure, only the x component of the force is shown.

Table 6: Modal damping values estimated by the EMA .

Frequency [Hz]	Modal Damping (%)
562	7.6
828	7.6
1221	3.7
1423	1.8
2154	0.5
2818	2.3

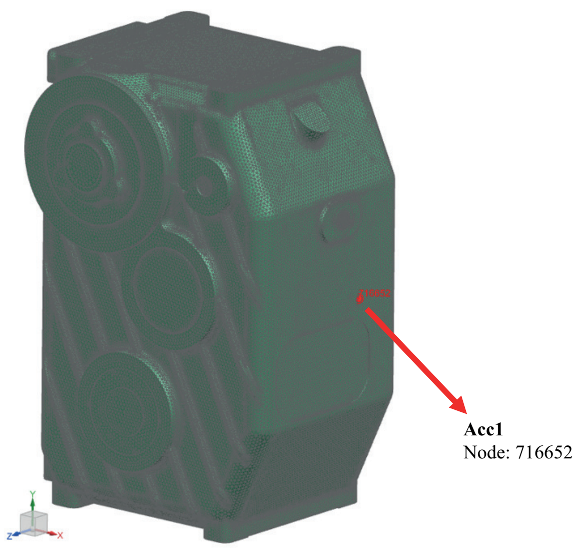

(a) Node corresponding to Acc1.

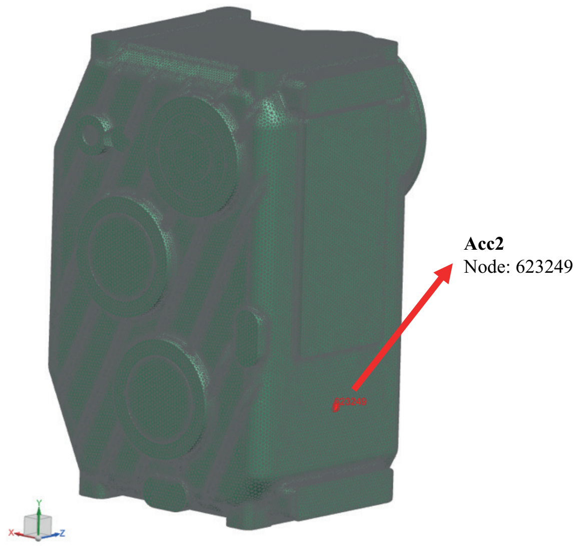

(b) Node corresponding to Acc2.

Figure 9: Location of the nodes corresponding to the two accelerometers Acc1 and Acc2.

Table 7: Reduction of the overall acceleration levels, x component, computed in the highest acoustic emission frequency range (562 - 2818 Hz). Reference acceleration is $a_{ref} = 1\ g$.

	Acc1		Acc2	
	Experimental	Numerical	Experimental	Numerical
dB reduction	-5.3	-7.3	-6.1	-5.5

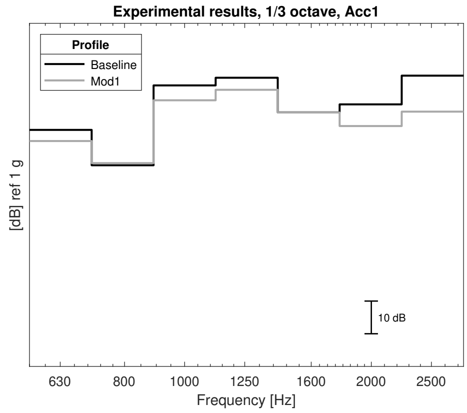

(a) Experimental results, Acc1.

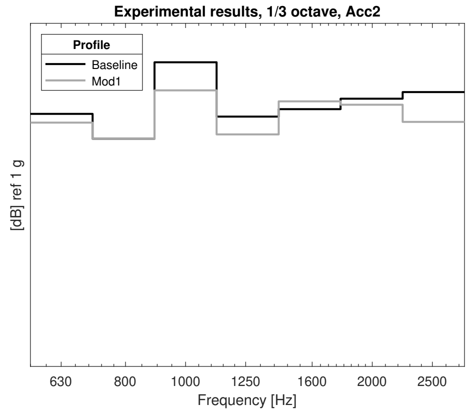

(b) Experimental results, Acc2.

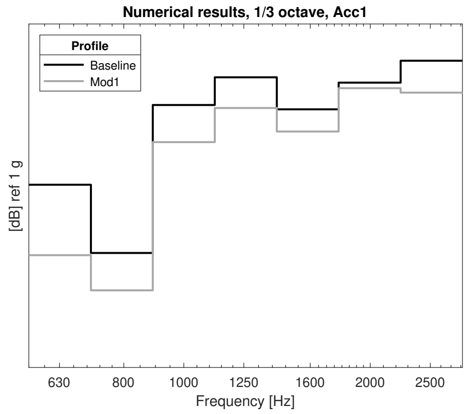

(c) Numerical results, Acc1.

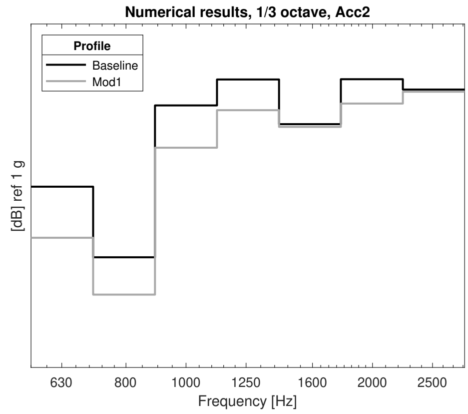

(d) Numerical results, Acc2.

Figure 10: Experimental and numerical acceleration levels in 1/3 octave band spectrum, x component, for both tooth profiles.

3.3 Acoustical finite-element model

An acoustical finite-element model is developed to estimate the overall acoustic level due to the vibration of the case, generated by gear meshing. The proposed AFE model exploits the acoustic transfer vector (ATV) methodology. This method consists in computing a set of functions which establish a relationship between the normal velocity of the nodes on the surface of the vibrating structure and the acoustic pressure at defined locations [9], called microphone points. For each one of them, a vector $\{ATV(f)\}$ is computed so that:

$$p(f) = \{ATV(f)\}^T \{v_n(f)\} \tag{4}$$

where $p(f)$ is the pressure at a specified location and $\{v_{n(f)}\}$ is a vector containing the normal velocities of each node on the radiating surface. All these quantities are frequency dependent. Assuming that there are m

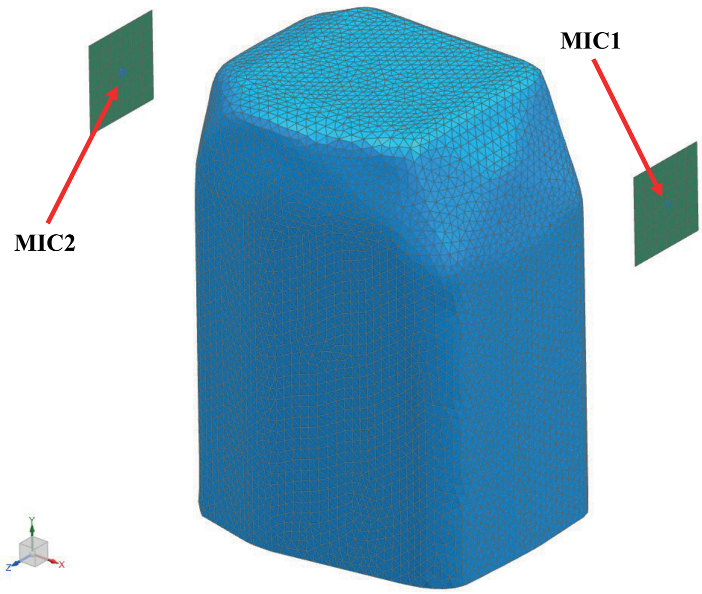

Figure 11: Acoustic mesh and microphone points.

microphone points and n nodes on the vibrating surface, the vector $\{ATV(f)\}$ is computed for all m point, so as to generate an $m\ x\ n$ ATV matrix $[ATM(f)]$ that satisfies the equation

$$\{p(f)\} = [ATM(f)]\{v_n(f)\} \tag{5}$$

where $\{p(f)\}$ is a vector of length m containing the frequency-dependent acoustic pressures at each microphone point. The main characteristic of the ATV matrix $[ATM(f)]$ is that it does not depend on the structural response, as it depends only on the properties of the acoustic domain and on the position of the microphone points. This means that the ATV matrix is constant and needs to be computed only once, provided that the fluid - radiating surface interface does not change, allowing to test various loading conditions, i.e. different case vibrations, using the same ATV matrix. This matrix can be computed using the Nastran solution SOL 108. In order to do so, it is necessary to create a 3D acoustic mesh for the fluid surrounding the gearbox case (Figure 11). As the problem concerns the solution of exterior acoustics, the size of the domain is reduced by exploiting a perfectly matched layer (PML), which is an artificial layer that absorbs all the incoming incident waves instead of reflecting them back into the fluid, independently from their frequency and their direction [10]. The PML allows to truncate the size of the acoustic domain, thus reducing the number of 3D elements needed to create the mesh. Considering Figure 11, the layer is generated on the entire external surface of the mesh excluding its bottom side. On it, in fact, an infinite plane is defined to take into account the presence of the steel plate located below the case (Figure 2). Since it is a reflecting surface, a symmetric boundary condition is imposed on it, meaning that the normal velocity must be zero on the infinite plane. Microphone points, then, can be placed anywhere outside the layer, as shown in Figure 11. In the acoustic model, they are located in the same location as the corresponding microphones in the experimental tests. The acoustic fluid is assumed to be air having density $\rho = 1.20\,kg/m^3$ and speed of sound $c = 343\,m/s$

Once the ATV matrix has been computed, it can be combined with the results of the dynamic model to obtain the acoustic pressure at locations Mic1 and Mic2. The reductions of overall acoustic pressure levels due to to teeth profile modification are reported in Table 8. Moreover, Figure 12 compares the experimental and numerical results in 1/3 octave band spectrum. According to these results, the model is perfectly able to capture the relative reductions of the acoustic pressure when the tooth profile is changed. In fact, for Mic1 the reduction is 3.5 dB(A) for the experimental and -3.3 dB(A) for the numerical model. Moreover, for Mic2 the same reduction (-4.9 dB(A)) is achieved for both the experimental and the numerical results. This ensures the quality of the results obtained by the combined LP/SFE/AFE model. Hence, the proposed digital twin for the gearbox is validated.

Table 8: Reduction of the overall acoustic pressure levels, A-weighted, computed in the highest acoustic emission frequency range (562 - 2818 Hz). Reference pressure is $p_{ref} = 2 \cdot 10^{-5}\ Pa$.

	Mic1		Mic2	
	Experimental	Numerical	Experimental	Numerical
dB(A) reduction	-3.5	-3.3	-4.9	-4.9

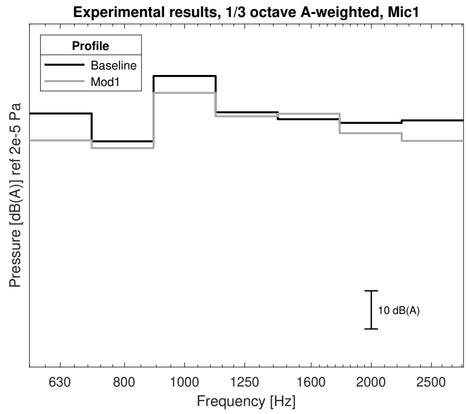

(a) Experimental results, Mic1.

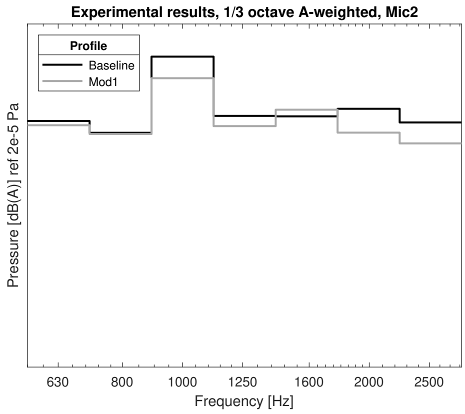

(b) Experimental results, Mic2.

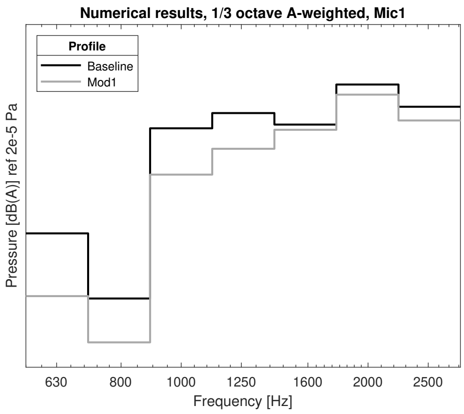

(c) Numerical results, Mic1.

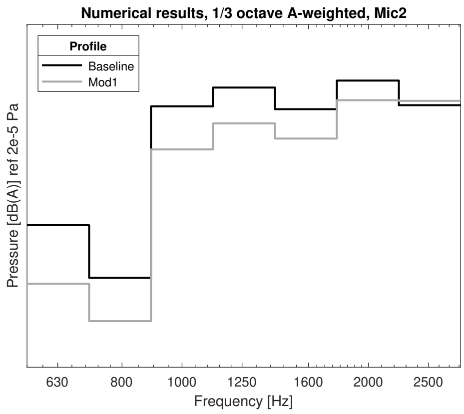

(d) Numerical results, Mic2.

Figure 12: Experimental and numerical A-weighted acoustic pressure levels in 1/3 octave band spectrum, for both tooth profiles.

4 Final remarks and further developments

In this work, a combined LP/SFE/AFE model for vibro-acoustic analysis has been presented. The model is exploited to generate the NVH digital twin of a real gearbox employed on agricultural equipment. The lumped parameter model simulates the dynamic behavior of the component inside the case; the structural finite-element model allows to predict its vibration; the acoustical finite-element model determines the overall acoustic pressure level at microphone points. Results have been experimentally assessed, and a good accordance is found between the numerical and the experimental data. In fact, the SFE model of the case accurately identifies the first two natural frequencies in the highest acoustic emission interval (Table 5). Furthermore, the dynamic SFE model is capable of capturing the reduction of overall accelerations levels due to different teeth profiles (Table 7), and so the AFE model in terms of overall acoustic pressure level (Table 8). The validation process allows to assert the combined LP/SFE/AFE model as a digital twin of the gearbox, hence a tool that may accompany the designer in the choice of the optimal solution for the noise generation problem. The main advantage of this model is the capability of being able to easily estimate the acoustic pressure level generated by various working conditions, i.e. input speeds and power, gear ratio and teeth profiles, in order to choose the optimal design which reduces the noise produced by gear meshing. In fact, by using the ATV method, once the ATV matrix has been computed, it does not need to be calculated again if the fluid-radiating surface interface does not change (i.e the external geometry of the case is not modified). This methodology speeds-up the optimization process since only the LP and the SFE models have to be solved to obtain the normal velocities on the surface of the case that are needed to estimate the acoustic pressure through the AFE model. Also, even the numerical modal analysis (SOL 103) has to be performed only once: in fact, once the structural mesh is validated, there is no need to carry it out again as the mesh of the case does not change. It is worth noting that the model is suitable to estimate overall levels and it can be employed as an instrument to evaluate the best design among a set of possible combinations of gear types to determine which one generates the lowest noise. Its main strength, in fact, resides in the capability to assess the variations in terms of dB when the magnitude of the excitation source, i.e. gear meshing, changes. Concerning possible further developments, the LP model should be extended in order to consider the gear ratio $\tau = 1.8$, as for this work it has been developed only to solve the case in which $\tau = 1$.

Acknowledgements

The authors would like to thank Comer Industries for the opportunity to apply this technique, as well as the logistic to make it happen. The innovative approach they have demonstrated in moving towards such methodology is quite remarkable. A special thanks to E. Fava for the support.

References

[1] J. Tuma. “Gearbox noise and vibration prediction and control”. In: *International Journal of Acoustics and Vibrations* 14.2 (2009), pp. 99–108.

[2] A. El Saddik. “Digital Twins: The Convergence of Multimedia Technologies”. In: *IEEE MultiMedia* 25 (Apr. 2018), pp. 87–92.

[3] E. Mucchi and G. Dalpiaz. “Numerical vibro-acoustic analysis of gear pumps for automotive applications”. In: *International Conference on Noise and Vibration Engineering 2012, ISMA 2012, including USD 2012: International Conference on Uncertainty in Structure Dynamics*. Vol. 5. 2012, pp. 3951–3961.

[4] E. Mucchi, A. Rivola, and G. Dalpiaz. “Modelling dynamic behaviour and noise generation in gear pumps: Procedure and validation”. In: *Applied Acoustics* 77 (Mar. 2014), pp. 99–111.

[5] Y. Guo et al. “Vibro-acoustic propagation of gear dynamics in a gear-bearing-housing system”. In: *Journal of Sound and Vibration* 333.22 (2014), pp. 5762–5785.

[6] Siemens PLM Software Inc. *Simcenter 3D*. Version 2019.2. 2019.

[7] The MathWorks Inc. *MATLAB*. Version 2018b. 2018.

[8] A. Kahraman and R. Singh. “Non-linear dynamics of a spur gear pair”. In: *Journal of Sound and Vibration* 142.1 (1990), pp. 49–75.

[9] R. Citarella, L. Federico, and A. Cicatiello. “Modal acoustic transfer vector approach in a FEM–BEM vibro-acoustic analysis”. In: *Engineering Analysis with Boundary Elements* 31.3 (2007), pp. 248–258.

[10] F. Hastings, J. Schneider, and S. Broschat. “Application of the perfectly matched layer (PML) absorbing boundary condition to elastic wave propagation”. In: *The Journal of the Acoustical Society of America* 100.5 (1996), pp. 3061–3069.